

# Design Of Positive Output Boost Converter With Integration Of Buck Converter For Reliable Electric Vehicle Battery Charging Application

1<sup>st</sup> Dr.B.Vijaya Krishna  
Assistant.Professor  
dept. of EEE  
Bapatla Engineering College  
Bapatla,India

2<sup>nd</sup> Dr. CH.Hariprasad  
Assistant.Professor  
dept.of EEE  
Bapatla Engineering College  
Bapatla,India

3<sup>rd</sup> S.Sujatha  
dept.of EEE  
Bapatla Engineering College  
Bapatla,India

4<sup>th</sup> p.jahnavi  
dept.of EEE  
Bapatla Engineering College  
Bapatla,India

5<sup>th</sup> v.sriram  
dept.of EEE  
Bapatla Engineering College  
Bapatla,India

6<sup>rd</sup> S.libnijoel  
dept.of EEE  
Bapatla Engineering College  
Bapatla,India

dept.of EEE Bapatla Engineering College

dept.of EEE Bapatla Engineering College

**Abstract**—DC-DC converters are essential to the use of electric vehicles (EVs). These days, EVs need a different DC-DC converter to charge their high- and low-voltage batteries. The performance of EVs may be impacted by these variables, which have also increased output voltage ripples, switching, and device conduction losses. Furthermore, the prior multiport EV applications, converters feature a greater number of switching and energy storage components. This article suggests a multiport DC-DC converter EV charging circuit to address these problems. The suggested circuit is a single-input dual-output (SIDO) design that combines a buck converter integration with a positive output boost converter (POBCIBC). In this case, the voltage is stepped down using a buck converter and stepped up using a POBC. A basic structure made up of Cascaded Boost Super Lift Luo Converters is called the POBC. The POBCIBC design offers a number of benefits compared to the current multiport converters, such as less storage components, a compact construction, high-voltage transfer gain, proficient efficiency, decreased switching and conduction losses, and reduced output voltage ripples. By building the MATLAB/Simulink and prototype models, the POBCIBC's performance is evaluated under various operating situations. Various output voltage levels have been created by the suggested converter according to variations in their duty cycles. The findings are displayed to demonstrate the EV application's proficient POBCIBC.

**Index Terms**—DC-DC Converter, voltage gain, single input dual output

## I. INTRODUCTION

Because they reduce emissions and rely less on fossil fuels, electric vehicles (EVs) can be extremely helpful in the global fight against climate change. The principal elements of electric vehicles (EVs) include the battery, control unit, DC-DC converters, inverter, electrical equipment, and

battery management system (BMS). In addition to raising the high voltage from low-voltage renewable energy sources, the DC-DC converter is utilized to charge the battery in electric vehicles [1, 2]. Nevertheless, the low- and high-voltage batteries in current EVs were charged using separate DC-DC converters, which can lead to higher switching losses, more output voltage ripples, significant conduction losses, and a decline in system efficiency. The EVs' performance is impacted by these problems. This article presents a single-input and multi output (SIMO) DC-DC converter for EVs as a solution to these problems. Favorable outcome in this article, a SIMO converter is defined as a put boost converter (POBC) with integrated buck converter (POBCIBC) operating in continuous conduction mode (CCM) with variable duty cycles. In this article, low voltage is handled by a stepping down converter and high voltage is handled by a POBC. In terms of voltage transfer gain (VTG), tenacity, and ripple voltage, the POBCIBC performs better than the current multi port DC-DC converters used for EV battery charging [3, 4]. The Luo converter for EV use, which integrates a buck converter, is well-done [5]. But this converter's effectiveness has generated 94.2 percentage. Well-presented is the brush less DC motor drive for EV that is powered by a DC-DC converter at low power levels [6]. For this task, the converter's efficiency is low, though. These days, multi-input and multi-output (MIMO) DC-DC converters are all the rage in electric vehicles. A well-executed SIMO transformer-based DC-DC converter with variable output voltage is [8]. Nevertheless, this converter had a number of problems that might have decreased its efficiency, including a large transformer size, increased cost, a greater number of power switches, larger on-off losses, and a complex control and driving circuit. A well-presented SIMO

Identify applicable funding agency here. If none, delete this.

with a connected inductor is [9]. A SIMO converter based on soft switching has been documented in [10]. But as a result of these experiments, coupled inductors have increased leakage current, increased on-off losses, and necessitated more intricate design procedures. A thorough analysis of the improved buck-boost DC-DC converter has been conducted [11]. This article claims that the converter's three switches, which use hard switching techniques to calculate the lower and maximum surge inductor currents, are designed for small power applications. There has been extensive reporting on the design of sliding mode controllers (SMC) for multi phase charger and discharge bidirectional DC-DC converters [12].

According to this experiment, during load changes, the inductor current of this converter with this control has resulted in peak overshoots of 1 V and ripple currents of 1.58 A. Additionally, the converter's design features a more intricate construction and only charges one battery. For low-voltage battery charging in electric vehicles, the zero voltage switching (ZVS) DC-DC converter with IC UCC389 control is well-presented [13]. Nevertheless, the intended converter resulted in 20 W of conduction losses when charging a single battery with a complicated structure. In addition, because of the higher power losses, phase shifter integrated circuits are quite expensive. A thorough examination of a five-stage DC-DC boost converter With a series LC for electric vehicle in real time is provided [14]. Nonetheless, this converter contains eight diodes and ten capacitors in addition to one inductor as storage components. Likewise, this converter's output voltage has produced peak overshoots of 34.9percent and a 100 ms settling period. The specifications of several DC-DC converters have been documented in [15], along with an evaluation of their performance and control strategies for EVs. converter has moderately efficiently charged one battery. There has been discussion on the Super Lift Luo Converter with buck converter integration for EV [17]. However, using two switches, two inductors, three capacitors, and three diodes, this converter has generated a 98percent efficiency. The thorough comparison of the suggested POBCIBC with earlier converters research gaps for EV applications is shown in Table 1. These studies clearly show that, in comparison to the current converters, the suggested POBCIBC obtained efficiency of 99.39percent with the fewest amount of elements. The literature analysis indicates that no POBCIBC design with duty cycle control has been documented for use in EV battery charging applications. Therefore, the goal of this article is to design the POBCIBC for use in electric vehicles. By creating the prototype and MATLAB/Simulink models, the entire model is validated under various working situations. The primary goals of this paper follows: (i) The duty is first determined, followed by the VTG and design equations for the POBCIBC's component parts.

(ii) The converter's cycles are adjusted to produce a broad variety of controlled output voltages. Next, by building the Simu link and experimental models, the POBCIBC is evaluated at various duty cycles and load resistance changes.

(iii) Lastly, the efficiency study at various converter param-

eter modifications, output voltage ripples, and time domain specification have all been used to analyze the results of the suggested converter. The structure of this article is as follows: The introduction, literature review, and primary goals of this work are covered in Section 1. The functioning and mathematical VTG of POBCIBC are covered in Sections 2 and 3. Section 4 outlines the suggested formulae for converter component designs. The computation of efficiency is carried out in Section 5. The findings and discussions of POBCIBC under various operating conditions are presented in Section 5. In Section 6, conclusions and upcoming projects are listed.

## II. PROPOSED POBCIBC WORKING

In Figure 1, the POBCIBC for EV application is shown. It consists of the input voltage  $V_{in}$ , two MOSFET switches  $S_1$ ,  $S_2$ , and storage elements including power transfer diodes  $D_1$ ,  $D_2$ , load resistors  $R_{o1}$ ,  $R_{o2}$ , and inductors  $L_1$ ,  $L_2$ , and capacitors  $C_{o1}$ ,  $C_{o2}$ . The POBCIBC's primary features are its single input and two output voltages at various levels. This POBCIBC is better suited as a power supply for different EV components. The POBCIBC's low-output voltage ( $V_{o2}$ )

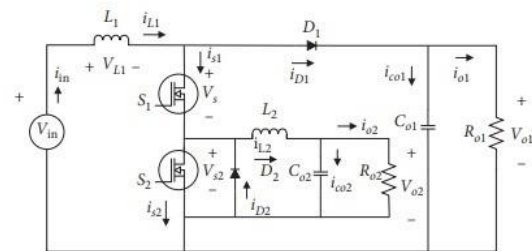


Fig. 1. Structure of the proposed POBCIBC

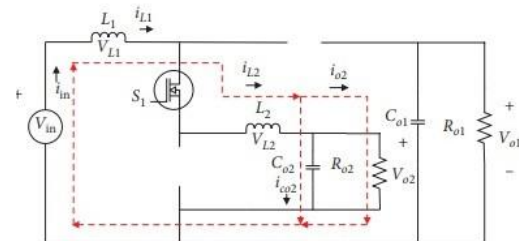


Fig. 2. (a) Modes 1 and 3

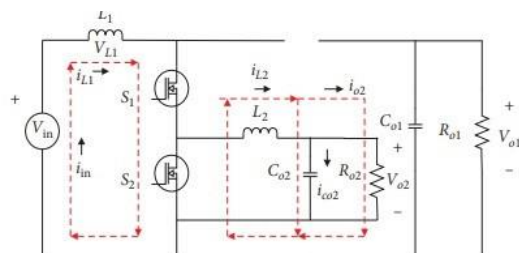


Fig. 3. (b) Mode 2

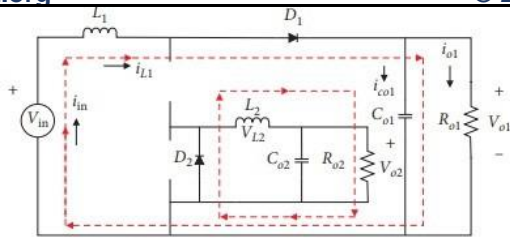


Fig. 4. (c) Modes 4

can be produced with the aid of a buck converter, but its output voltage (Vo1) has been enhanced with the use of a boost converter. POBCIBC has excellent In combination with conventional multiport converters, KY converters, and SEPIC, VTG offers reduced circuit components, low current and voltage ripples, a simple structure, good power density, and efficiency. The POBCIBC operates in four distinct modes, each of which is represented by an equivalent circuit in Figure 2(a)–2(c). **Referring to Figure 2(a), Mode 1 (0 ; t ; t1):** S1 is closed and S2 is open when operating in Mode 1. In order to energize inductor L2 in this mode and supply the buck load Ro2, the stored energy from inductor L1's prior mode is de-energized. This mode ends following the (d1-d2/2)Ts interval of time. Because of the resonance path between the L1, L2, and Co2 during the previous switching state time interval, the S1 voltage is zero. In addition, the D1 and D2 are operating in reverse polarization.

$$V_{s1/s2/D1/D2-stress} = V_{o1} - V_{in} \cdot \tag{1}$$

**(2) Check out Mode 2 (t1 ; t ; t2) in Figure 2(b):** S1 is open and S2 is closed when operating in Mode 2. To load Ro2, the inductor L2 releases its stored energy. Vin also provides L1 with energy. In this mode, the D2 is inversely polarized. This mode's time interval is d2Ts time interval.

$$\begin{aligned} i_{s1/s2-stress} &= i_{in} \\ i_{D1-stress} &= i_{o1} \\ i_{D2-stress} &= i_{o2} \end{aligned} \tag{2}$$

**Referring to Figure 2(a), Mode 3 (t2 ; t ; t3):** This mode operates in the same way as Mode 1. **Referring to Figure 2(c): Mode 4 (t3 ; t ; t4):** S1 and S2 are in open states in this mode. Energy from L1 and L2 is released to power Ro1 and Ro2 loads.

$$\begin{aligned} V_{o1} &= V_{in} - V_{L1} \\ V_{o2} &= -V_{L2} \\ i_{L1} &= i_{Co1} + V_{o1}/R_{o1}. \end{aligned} \tag{3}$$

### III. EFFICIENCY COMPUTATION

When determining the converter efficiency, the element losses are taken into account. Equation is how it is written.

$$\eta = P_o / (P_o + P_{Losses}) \tag{4}$$

Name of the parameters	Symbols	Value	
Duty cycles	$d_1$	0.6	0.9
	$d_2$	0.3	0.8
Input voltage	$V_{in}$	12 V	12 V
Output voltages	$V_{o1}$	17.14 V	60 V
	$V_{o2}$	5.14 V	6 V
Load resistances	$R_{o1}$	25 $\Omega$	
	$R_{o2}$	12.5 $\Omega$	
Load currents	$i_{o1}$	0.6856 A	2.4A
	$i_{o2}$	0.4112 A	0.48A
Input current	$i_{in}$	0.985 A	13.633A
Efficiency	$\eta$	99.39%	89.78%
Output powers	$P_{o1} + P_{o2}$	11.75 W	146.88 W
Input power	$P_{in}$	11.82 W	163.5 W
Switching frequency	$f_s$	30 kHz	
Inductors	$L_1$ and $L_2$	3.2 and 2 mH	
Output capacitors	$C_{o1} = C_{o2}$	3 $\mu$ F	
Capacitors ripple voltage	$\Delta V_{Co1}$ and $\Delta V_{Co2}$	1 and 0.1 V	

Fig. 5. Specification of POBCIBC for EV application.

Next, we can express the converter's overall power losses using Equation

$$P_{Losses} = P_{Switches} + P_{Diodes} + P_{Capacitors} + P_{Inductors} \tag{5}$$

The switching power losses are calculated during on and off conditions

$$P_{Switches} = P_{S, on} + P_{S, off} / 2 \tag{6}$$

the switching power losses in on/off operating conditions are evaluated.

$$\begin{aligned} P_{S1, on} &= r_{on} i_{in}^2 d_1 \\ P_{S2, on} &= r_{on} i_{in}^2 d_2 \\ P_{S, off} &= f_s C_{os} V_{S-stress}^2 \end{aligned} \tag{7}$$

Diode conduction and non conduction state losses are calculated with help of Equations

$$\begin{aligned} P_{D1, on} &= r_f i_{in}^2 (1 - d_1), \\ P_{D1, off} &= V_f i_{in} (1 - d_1) \end{aligned} \tag{8}$$

where rf is diode forward resistance and Vf is threshold or forward voltage of the diode.

$$\text{Total diode losses, } P_{Diodes} = P_{D1, on} + P_{D1, off} \tag{9}$$

Storage elements power losses are computed by using Equations

### IV. RESULTS AND DISCUSSIONS

The computational and experimental responses of the POBCIBC for EV applications at different load operating circumstances are described in this section along with the corresponding specifications. table 2's converter catalog. The specifications of the D1, D2-UF5803, inductors, L1, L2-Ferrite core (10 6832 driver circuit. The gate and source of switches S1 and S2 are then connected to the driver IC outputs in order to control the output voltages with various duty cycles. The experimental

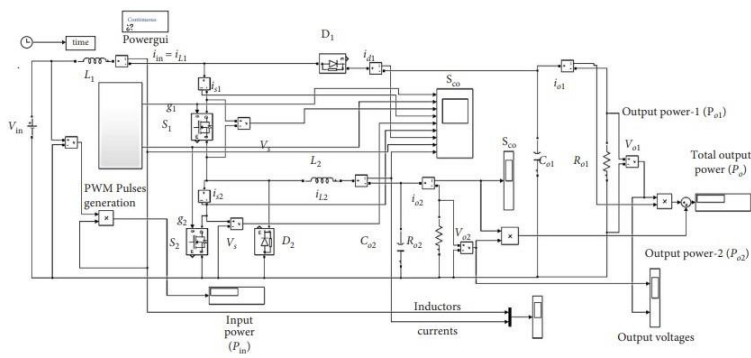


Fig. 6. MATLAB/Simulink model for the proposed POBCIBC (a)

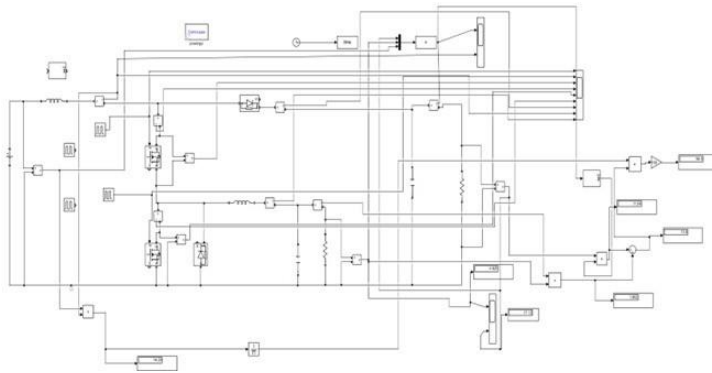


Fig. 7. Designed simulation

and simulated responses of the output voltages,  $V_{in}$ , and PWM pulses of the proposed POBCIBC with duty cycles of switches  $d_1=60$  Figures 6(a) and 6(b). With minor overshoots and a short setting time of 0.001 s, it is evident from these statistics that the POBCIBC output voltages,  $V_{o1}=17.14$  V and  $V_{o2}=5.14$  V, match theoretical values (see Table 2). Furthermore, output voltages of the suggested Little waves have been seen in the modeling and experimental responses from the converter. The output's experimental and simulation responses are displayed in Figures 7(a) and 7(b). voltages, PWM pulses, and input voltage of the suggested POBCIBC with  $d_1=90$  percent and  $d_2=80$  percent and  $V_{in}=12$  V. These figures clearly show that

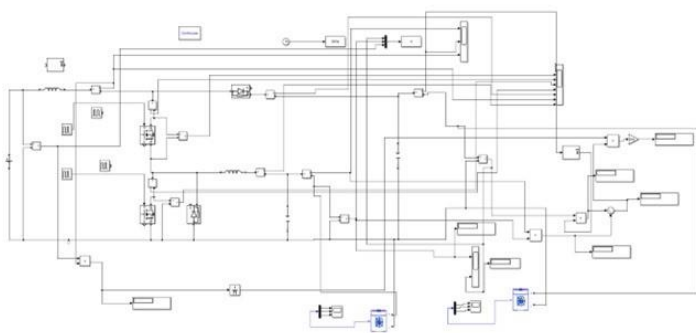


Fig. 8. Battery Connected Simulation Diagram

the output voltages of the POBCIBC have  $V_{o1}=60$  V and  $V_{o2}=6$  V, low overshoots, and a setting time of 0.02 s in both the experimental and simulation responses. Moreover, the simulation and experimental analyses of the suggested converter's  $V_{o1}$  and  $V_{o2}$  have shown minimal ripples. The actual and simulation results closely align with the theoretical values (Table 2). capacitors,  $C_{o1}, C_{o2}$  -electrolytic type PIC 18f6310 (PC1, PC2, and 32 MHz) and IC-Fan 6832 driver with circuit for amplification. The prototype model of the same converter is shown in Figure 5(b), whereas Figure 5(a) shows the Simulink model POBCIBC. The PIC18f6310 is utilized to create PWM pulses for the converter's switches. After that, it is used to isolate the power and control units on Fan 6832 driver circuit. POBCIBC. The PIC18f6310 is utilized to create PWM pulses for the converter's switches. After that, it is used to isolate the power and control units on Fan 6832 driver circuit. The gate and source of switches it is used to isolate the power and control units on Fan converter circuit are as follows: Microcontroller-based pulse width modulation (PWM) generation using MOSFTE IRFN 540 switches  $S_1-S_2$ , diodes,  $D_1, D_2$ -UF5803, inductors,  $L_1, L_2$ -Ferrite core (10 6832 driver circuit.

Little waves have been seen in the modeling and experimental responses from the converter. The output's experimental and simulation responses are displayed in Figures 7(a) and 7(b). voltages, PWM pulses, and input voltage of the suggested POBCIBC with  $d_1=90$  and  $d_2=80$  percentage  $V_{in}=12$  V. These figures clearly show that the output voltages of the POBCIBC have  $V_{o1}=60$  V and  $V_{o2}=6$  V, low overshoots, and a setting time of 0.02 s in both the experimental and simulation responses. Moreover, the simulation and experimental analyses of the suggested converter's  $V_{o1}$  and  $V_{o2}$  have shown minimal ripples. The actual and simulation results closely align with the theoretical values (Table 2). Figures 8(a) and 8(b) depict the POBCIBC simulated gate pulses, voltage across the switches, and current through the switches/inductors/diodes responses with  $V_{in}=12$  V and  $d_1=60$  and  $d_2=30$  percent at different load resistance. It is found that the voltage across the switches, current through the switches, inductor, and diodes of the designed POBCIBC has no voltage and current stresses during the converter operation. When the inductor currents remained constant, the POBCIBC was also running in continuous conduction mode (DCM) or continuous CCM. The theoretical key waveform is represented by all of the parameters (see Figures 3 and 8). Both the theoretical and experimental numerical values for POBCIBC at rated load circumstances are shown in Table 3. These results demonstrate that the suggested POBCIBC has created minimal ripples of the output voltages (1.2 V )(simulation), 1.6 V (experimental), and 0.005 V (simulation), 0.0007 V, and efficiency of 99.39 percent(simulation) and 98.49 percent (experimental) at load of  $R_{o1}=25$  and  $R_{o2}=12.5$  . suggested POBCIBC for EV applications using earlier converters. These studies clearly show that, compared to the current converters, the suggested POBCIBC obtained an efficiency of 99.39 percent with the fewest amount of components (see Table 3, bolded). Equations (14)–(25) are

used in Figure 9 to display the percentages of loss breakdown at almost full load for the different POBCIBC components. Consequently, semiconductor device losses account for the majority of power losses. It should be mentioned that the switches' and diodes conduction losses becomes dominant because of the large current flowing through them in the output powers and high-voltage gains. Thus, low-on-resistance, high-power semiconductors to be used to raise the converter's efficiency. conduction losses becomes dominant because of the large current flowing through them in the output powers and high-voltage gains. Thus, low-on-resistance, high-power semiconductors to be used to raise the converter's efficiency.

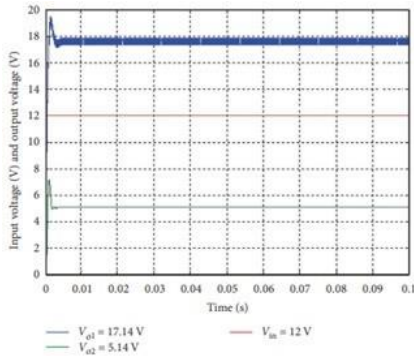


Fig. 9. : Simulated and experimental results of POBCIBC, (a) d1=60 and d2=30percent (CH1 : 2 V/div; CH2 : 5 V/div-gate voltages of switches)

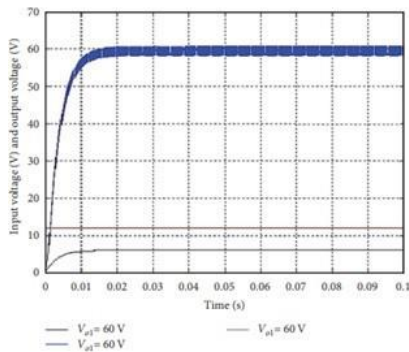


Fig. 10. input voltage and output voltages (CH1 : 10 V/div; CH2 : 10 V/div-output voltages; time: 20 μs/div))

the table shows the Simulated performance analysis of POBCIBC for EVs application at rated load operating condition with  $v_{in}=12V$  and different duty cycle

V. CONCLUSION

this article, the theoretical analysis, design and output voltage regulation of multi port POBCIBC operated in CCM using different duty cycle has been successfully demonstrated. The PWM pulses were generated using PIC18f6310 for POBCIBC. The main merits of the designed POBCIBC over the previous multi port converter as follows: (i) Obtain the good VTG and flexibility to change the different output voltages; (ii) Excellent

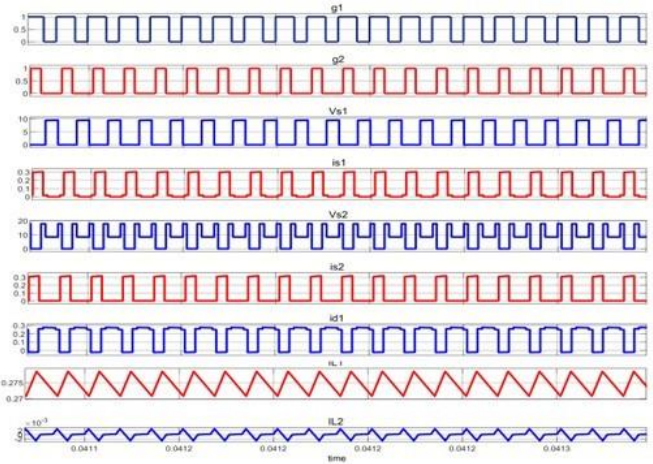


Fig. 11. designed Simulated current and voltage variations waveform for various elements of proposed POBCIBC (Ro1=12.5 and Ro2=50 ))

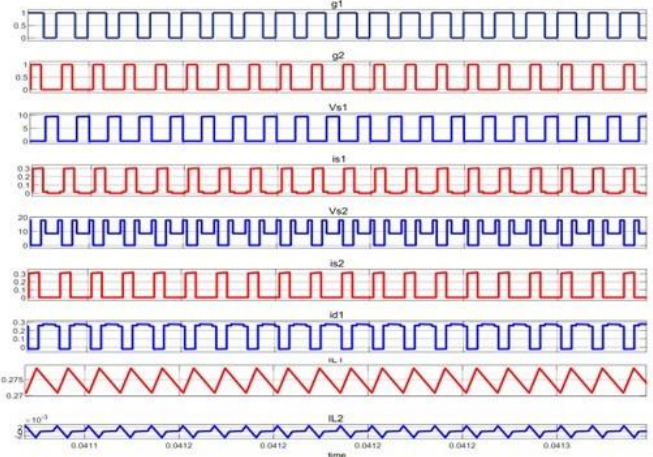
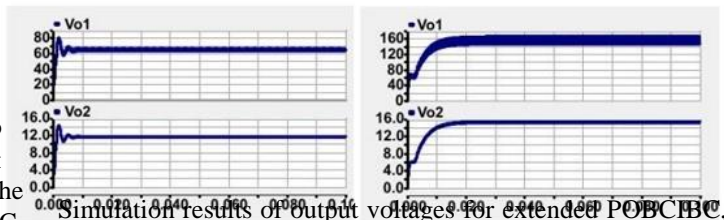


Fig. 12. designed Simulated current and voltage variations waveform for various elements of proposed POBCIBC (Ro1=50 and Ro2=100 ))



Simulation results of output voltages for extended POBCIBC, (a) D2 = 30 and D1 = 60percent (b) D2 = 80 and D1 = 90percent)

Ro1 ()	Ro2 ()	Efficiency
25	12.5	99.39
50	25	95.48
100	50	91.22
150	75	87.98
200	100	85.11
250	125	82.49

Fig. 13.

efficiency like 99.39percent (iii) Minimal output ripple voltages as well as inductor ripple currents; (iv) Simple structure and less number of components; and (v) Low conduction and switching losses. The experimental and simulation results are presented in order to prove the competence of the designed multi port POBCIBC at different load and duty cycle operating conditions. It is, therefore, mainly designed for EV battery charging application. In future, multi port converter based LUO and KY topologies to be built for EV and renewable energy application.

#### REFERENCES

- [1] J. S. Habib, M. M. Khan, F. Abbas et al., "Contemporary trends in power electronics converters for charging solutions of electric vehicles," *CSEE Journal of Power and Energy Systems*, pp. 1–36, 2020.
- [2] J. J. A. Alahyari, M. Fotuhi-Firuzabad, and M. Rastegar, "Incorporating customer reliability cost in PEV charge scheduling schemes considering vehicle-to-home capability," *IEEE Transactions on Vehicular Technology*, vol. 64, no. 7, pp. 2783–2791, 2015.
- [3] B.-R. Lin, "DC–DC converter implementation with wide output voltage operation," *Journal of Power Electronics*, vol. 20, pp. 376–387, 2020.
- [4] J. F.-L. Luo and Y. Hong, *Advanced DC/DC Converters*, PCRC Press and Taylor and Francis Group, London, New York, 2006.
- [5] J. S. K. Ramu, R. K. Balaganesh, S. K. Paramasivam et al., "A novel high-efficiency multiple output single input step-up converter with integration of Luo network for electric vehicle applications," *International Transactions on Electrical Energy Systems*, vol. 2022, Article ID 2880240, 13 pages, 2022.
- [6] R. Ashokkumar, M. Suresh, B. Sharmila et al., "A novel method for Arduino based electric vehicle emulator," *International Journal of Ambient Energy*, vol. 43, no. 1, pp. 4299–4304, 2022.
- [7] G. Balan, S. Arumugam, S. Muthusamy et al., "An improved deep learning-based technique for driver detection and driver assistance in electric vehicles with better performance," *International Transactions on Electrical Energy Systems*, vol. 2022, Article ID 8548172, 16 pages, 2022.
- [8] G. Chen, Y. Liu, X. Qing, M. Ma, and Z. Lin, "Principle and topology derivation of single-inductor multi-input multioutput DC–DC converters," *IEEE Transactions on Industrial Electronics*, vol. 68, no. 1, pp. 25–36, 2020.
- [9] P. KhademiAstaneh, J. Javidan, K. Valipour, and A. Akbarimajd, "A bidirectional high step-up multi-input DC–DC converter with soft switching," *International Transactions on Electrical Energy Systems*, vol. 29, no. 1, Article ID e2699, 2019.
- [10] G. Li, J. Xia, K. Wang, Y. Deng, X. He, and Y. Wang, "Hybrid modulation of parallel series LLC resonant converter and phase shift full-bridge converter for a dual-output DC–DC converter," *IEEE Journal of Emerging and Selected Topics in Power Electronics*, vol. 7, no. 2, pp. 833–842, 2019.
- [11] Z. Shen, X. Chang, W. Wang, X. Tan, N. Yan, and H. Min, "Predictive digital current control of single-inductor multipleoutput converters in CCM with low cross regulation," *IEEE Transactions on Power Electronics*, vol. 27, no. 4, pp. 1917–1925, 2012.
- [12] J. P. V. Ceballos, S. I. Serna-Garcés, D. G. Montoya, C. A. Ramos-Paja, and J. D. Bastidas-Rodríguez, "Charger/ discharger DC/DC converter with interleaved configuration for DC-bus regulation and battery protection," *Energy Science Engineering*, vol. 8, no. 2, pp. 530–543, 2020.
- [13] K. Sayed, "Zero-voltage soft-switching DC–DC converterbased charger for LV battery in hybrid electric vehicles," *IET Power Electronics*, vol. 12, no. 13, pp. 3389–3396, 2019.
- [14] H. Khalid, S. Mekhilef, M. B. Mubin et al., "Analysis and design of Series-LC-switch capacitor multistage high gain DC–DC boost converter for electric vehicle applications," *Sustainability*, vol. 14, no. 8, Article ID 4495, 2022.
- [15] A. Turksoy, A. Teke, and A. Alkaya, "A comprehensive overview of the DC–DC converter-based battery charge balancing methods in electric vehicles," *Renewable and Sustainable Energy Reviews*, vol. 133, Article ID 110274, 2020.
- [16] P. S. Tomar, M. Srivastava, and A. K. Verma, "An improved current-fed bidirectional DC–DC converter for reconfigurable split battery in EVs," *IEEE Transactions On Industry Applications*, vol. 56, no. 6, pp. 6957–6967, 2020.
- [17] B. Faridpak, M. Farrokhifar, M. Nasiri, A. Alahyari, and N. Sadoogi, "Developing a super lift Luo-converter with integration of buck converters for electric vehicle applications," *CSEE Journal of Power and Energy Systems*, vol. 7, no. 4, pp. 818–820, 2021.
- [18] I. A. Aden, H. Kahveci, and M. E. Şahin, "Design and implementation of single-input multiple-output DC–DC buck converter for electric vehicles," *Journal of Circuits, Systems and Computers*, vol. 30, no. 13, 2021.
- [19] D. Yu, J. Yang, R. Xu, Z. Xia, H. H.-C. Iu, and T. Fernando, "A family of module integrated high step-up converters with dual coupled inductors," *IEEE Access*, vol. 6, pp. 16256–16266, 2018.